HHS Public Access

Author manuscript

Arthritis Rheumatol. Author manuscript; available in PMC 2017 July 18.

Published in final edited form as:

Arthritis Rheumatol. 2016 May ; 68(5): 1301–1313. doi:10.1002/art.39538.

Contradictory role of CD97 in basal and tumor necrosis factor α-induced osteoclastogenesis in vivo

Hee Yeon Won, **Se Hwan Mun**, **Bongjin Shin**, and **Sun-Kyeong Lee**

UCONN Center on Aging, University of Connecticut Health Center, Farmington, CT 06030

Abstract

Objective—CD97, a member of the EGF-TM7 family of adhesion GPCR, is expressed on various cell types. We report here the contradictory role of CD97 in osteoclastogenesis in both basal and response to TNF treatment. We found that RANKL induced CD97 in FACS sorted osteoclast precursor cells. To elucidate the functions of CD97 in bone and inflammation, we examined the role of CD97 on osteoclastogenesis in vitro, the skeletal phenotype of CD97-deficient mice (CD97 KO), and responses to TNFα.

Methods—CD97 KO mouse model and TNF challenge were used to investigate the role in bone and inflammation in vivo. The effects of CD97 in bone and inflammation were assessed using histomorphometric analysis, in vitro cultures, RT-PCR and multiplex analysis of serum.

Results—In vitro, RANKL induced CD97 expression in bone marrow macrophages (BMM). In vivo, trabecular bone volume in the femurs of CD97 deficient female mice was increased and was associated with a decrease in osteoclast number. CD97 KO mice have reduced potential to form osteoclast-like cells (OCL) in vitro. Further, TNFα treatment augmented osteoclast formation in calvaria of CD97 KO mice in vivo by increasing the production of RANKL and other cytokines and chemokines and by reducing OPG by calvarial cells

Conclusion—Our findings demonstrate that CD97 is a positive regulator of OCL differentiation, influencing bone homeostasis. However, CD97 may be essential to suppress initial osteoclastogenesis in response to acute and local inflammatory stimuli.

INTRODUCTION

Bone homeostasis is tightly regulated by the bone-resorbing activity of osteoclasts (OCs) and the bone-forming activity of osteoblasts (OBs). Osteoclasts are large, multinucleated cells that are formed by the fusion of precursor cells of the monocyte-macrophage lineage (1, 2). The differentiation of functional OCs is principally regulated by macrophage colony-stimulating factor (M-CSF) and the receptor activator of NF-κB ligand (RANKL) (3–5). Binding of RANKL to its receptor, receptor activator of nuclear factor κB (RANK), activates a variety of transcription factors, including nuclear factor of activated T cells (NFAT) c1 and c-fos, leading to fully differentiated and functional osteoclasts (6).

Address for correspondence: Sun-Kyeong Lee, Ph.D., UCONN Center on Aging, MC1835, University of Connecticut Health Center, 263 Farmington Avenue, Farmington, CT 06030-1835, TEL: (860) 679-8177, FAX: (860) 679-8891, slee@uchc.edu.

Conflict of Interest: All authors have no conflict of interest.

CD97 is a member of the EGF-seven-span transmembrane (EGF-TM7) family of adhesion G protein coupled receptors (GPCRs) (7). Although originally identified as an early activation antigen on lymphocytes (8, 9), CD97 has been detected on almost all types of leukocytes, macrophages and dendritic cells. In particular, it is also expressed by normal epithelial, muscle, endothelial and fat cells in both humans and mice (10–14). While constitutively expressed in monocytes and macrophages (8), CD97 is present at low levels on resting lymphocytes, but is strongly up-regulated within a few hours after lymphocyte activation (10, 15). In synovial tissue sections from both rheumatoid arthritis and osteoarthritis, CD97 has been detected in all macrophages. In addition, high expression and elevated levels of soluble CD97 at sites of inflammation have been reported, suggesting a role for CD97 in immune responses (16–18).

Three ligands for CD97 have been identified in humans. These include integrins, αvβ1, and possibly αvβ3, which bind a RGD motif in the stalk region of the CD97 α chain (19), CD55, also known as decay accelerating factor (DAF), which interacts with EGF domains 1 and 2 of the extracellular α-chain (20) and the glycosaminoglycan chondroitin sulfate which binds the EGF domain 4 (21). In contrast, only CD55 has been identified as a CD97 ligand in mice (16, 22, 23). CD55 is a glycosylphosphatidylinositol (GPI)-anchored transmembrane protein. The adhesive interaction between CD97 and CD55 is independent of the RGD motif (22).

Tumor necrosis factor (TNF) is one of the most potent proinflammatory cytokines and can elicit the entire inflammatory cascade. TNFα is known to amplify osteoclastogenesis via mechanisms both independent and dependent of RANKL (24–26), and TNFα-induced RANKL synthesis by bone marrow stromal cells is a fundamental component of inflammatory osteolysis (27). RANKL dependent TNFα action has been reported to stimulate osteoclastogenesis by association of RANK and TNF type 1 receptor, and TNFα and RANKL synergistically upregulate RANK expression (28). In addition, synergistic effects between RANKL and TNFα directly induce bone marrow macrophage to commit to the osteoclast lineage (24). TNF has been also known to induce osteoclast recruitment (29) and can contribute further to bone loss by suppressing bone formation, in part, by the induction of osteoblast apoptosis (30, 31).

In the current study, we identified a novel role for CD97 in bone remodeling and the acute response to inflammation. We demonstrate that CD97 is a positive regulator of OCL differentiation. Further, CD97 may be essential to suppress osteoclastogenesis in the responses of bone to acute inflammatory stimuli, such as TNFα.

MATERIALS AND METHODS

Animals

Seven to eight week old wild-type (WT) and CD97-deficient (CD97 KO) mice in a C57BL/6 background were used throughout experiments. CD97-deficient mice (CD97^{tm1Dgen}/J) were purchased from The Jackson Laboratory, originally generated by Veninga et al (12), backcrossed to C57BL/6J for additional 7 generations and were housed at the University of Connecticut Health Center. Heterozygous CD97 KO mice were bred to generate littermate

WT and CD97 KO mice. Recombinant mouse TNFα (0.75 μg) was injected supracalvarially daily for 4 days before calvarial tissues were removed for histology, RNA and protein extraction. Animal handling and experiments were performed in accordance with the guidelines of Animal Care Committee of the University of Connecticut Health Center.

Reagents

Please see "Supplemental Materials"

Cell cultures and osteoclast measurement

Bone marrow cells were isolated from femur and tibia of WT or CD97 KO mice by a modification of previously published methods (32–34). Detailed experimental procedures can be found in "Supplemental Materials."

Colony-forming unit granulocyte-macrophage (CFU-GM) assay

Total bone marrow cells were plated on 35-mm tissue culture dishes in 1 ml 1.5 % methylcellulose supplemented with 20 % HIFBS, 2 % BSA and recombinant mouse granulocyte macrophage colony stimulating factor (GM-CSF) (1 ng/ml) as the source of colony stimulating activity. Cultures were maintained at 37°C for 7 days. The number of colonies containing more than 40 cells was counted at the end of incubation (35).

Flow cytometry

Single cell suspensions from bone marrow were incubated with various fluorochrome conjugated anti-CD3, anti-CD45R (B220), anti-CD11b (Mac-1), anti-CD117 (c-kit) and anti-CD115 (c-fms) antibodies for 40 min on ice following manufacturer's instructions. Cells were then washed with 1 HBSS containing 10 mM HEPES (pH7.4), 2 % HIFBS and analyzed by LSRII and FlowJo software from Tree Star, Inc. (Ashland, OR, USA). Specific osteoclast precursor population ($B220^{-}CD3^{-}CD11b^{-/lo}c\text{-}fms^{+}$) was sorted in a BD-FACS Aria (BD Biosciences, San Jose, CA, USA) equipped with five lasers and 18 fluorescence detectors for osteoclast formation assays in vitro.

Pit formation assay

To quantify resorption pit formation, cells were cultured in collagen gels in the presence of M-CSF and RANKL (both at 30 ng/ml) for 6 days. Fully differentiated multinucleated cells were removed by digestion with 0.1% collagenase and placed on UV-sterilized devitalized bovine cortical bone slices. Equal number (100 cells per bone slice) of cells were placed in a 96 well plate with M-CSF (30 ng/ml) and RANKL (30 ng/ml) for 24 hrs. The bone slices were sonicated in 0.25 M NH_4OH to remove osteoclasts. Bone slices were stained with 1 % toluidine in 1 % borax buffer to visualize resorption pits. The resorption pits were viewed under the light microscope (Olympus BX53) and were measured by Olympus CellSens imaging software.

Micro-CT and histomorphometric analyses

The femurs from WT and CD97 KO mice were removed and fixed in 70 % ethanol at 4 °C for micro-CT analysis (36). For static histomorphometry, mouse femurs were fixed in 4 %

paraformaldehyde (Sigma-Aldrich, St. Louis, MO, USA) prior to decalcification, embedded in paraffin and sectioned serially at 7 μm thickness, followed by staining with hematoxylin and eosin (H&E) or TRAP. Tissue sections were examined using a computerized semiautomated system (Osteomeasure, Nashville, TN, USA) with light microscope. The measurement terminology and units used for histomorphometric analysis were those recommended by the Nomenclature Committee of the American Society for Bone and Mineral Research (37).

For dynamic histomorphometry, WT and CD97 KO females mice received intraperitoneal injections of 10 mg/kg of calcein 9 days and 2 days before death. Bones were fixed for three to five days in 4% paraformaldehyde in PBS, decalcified, incubated in 30 % sucrose overnight and embedded in OCT compound (Thermo Fischer Scientific, Waltham, MA). Sections of 7 μm were obtained using a Leica cryostat (Wetzler, Germany) and tape transfer system (Section-lab, Hiroshima, Japan). Fluorescent images were obtained as previously described (38). Detailed experimental procedures, analyses and the regions of interest can be found in “Supplemental Materials.”

Western blot analysis

BMM cells (5×10^5 cell/well in 6 well plate) were treated with M-CSF for 3 days before the cells were treated with RANKL for the period indicated in each experiment. Cells were lysed in cold lysis buffer and quantified. Equal amounts of whole cell lysates were loaded and electrophoresed on SDS-PAGE using 10 % running gel under reducing conditions. Separated proteins were transferred to nitrocellulose membrane and membranes were probed with anti-NFATc1, anti-c-fos, anti-IκBα, anti-phospho-c-jun, anti-CD97 or anti-β-actin antibody.

Reverse Transcription and real time PCR

Detailed experimental procedures and information on the specific primers can be found in “Supplemental Materials.”

Statistical analysis

Statistical analysis was performed by Student’s t-test or one way analysis of variance (ANOVA) and the Bonferroni post hoc test when ANOVA demonstrated significant differences. All experiments were repeated at least twice and representative experiments or pooled data are shown.

RESULTS

RANKL up-regulated CD97 expression

As we previously reported, a specific population of FACS sorted mouse bone marrow cells ($B220^-CD3^-CD11b^{-/lo}c\text{-}fms^+$) can differentiate into multinucleated osteoclasts with high efficiency (39, 40). We FACS sorted this population from mouse bone marrow (flushed from femurs and tibia) and cultured it for 4 days with M-CSF with or without RANKL. We found that CD97 was induced by RANKL in these cultures (Fig. 1A). Figure 1B shows that CD97 expression was detected in freshly isolated osteoclast precursor population in the bone

marrow. We confirmed that CD97 expression was greater in M-CSF and RANKL treated bone marrow macrophage (BMM) cells compared to M-CSF treated controls. We examined the expression pattern of CD97 during RANKL-induced osteoclast differentiation by real time-PCR and western blot analysis. RANKL treatment increased CD97 mRNA (Fig. 1C) on day 2 of culture and peaked at day 5. CD97 protein levels were transiently induced on day 2 with RANKL, peaked on days 3 and 4, and rapidly decreased thereafter (Fig. 1D). These results suggest that RANKL up-regulates CD97 expression.

CD97 siRNA inhibits osteoclast formation

To investigate the role of CD97 in RANKL-mediated osteoclast differentiation, we utilized CD97 siRNA for loss of function experiments. BMM cells were transfected with the combination of 4 different CD97 siRNAs (Qiagen) or a negative control and cultured with M-CSF and RANKL. We confirmed that the siRNA specific to CD97 efficiently down regulated CD97 mRNA (Supplemental Fig. 1A) and protein (Supplemental Fig. 1B) levels. In addition, siRNA specific to CD97 down regulated the formation of TRAP(+) multinucleated cells compared to negative control siRNA as shown in Supplemental Figure 1C. Concurrently we determined that the knockdown of CD97 expression attenuated the expression of osteoclast differentiation markers NFATc1 and c-fos during RANKL-mediated osteoclastogenesis when compared to negative control (data not shown). These results strongly suggest that CD97 plays a positive role in osteoclast differentiation.

CD97 deficient mice have increased bone mass

We next examined if differences exist between the bones from WT and CD97 KO mice in vivo. We performed micro-CT analysis on 8 week old WT and CD97 KO mice. As shown in figure 2A and B, only female CD97 KO mice demonstrated significant differences in trabecular bone at this age. In female mice, bone volume (BV/TV) was increased in CD97 KO mice compared to WT mice, while there was no significant difference in male CD97 KO mice. Although we found no significant difference in cortical bone area in either males or females (data not shown) cortical thickness remained unaffected in female but increased in male CD97 KO mice (Fig. 2C). There was no significant difference in length and overall size of the femur by micro-CT including the length, endosteal and periosteal perimeters and sub-periosteal and sub-endosteal area. Since the trabecular bone is the most metabolically active compartment, and the trabecular bone phenotype was observed in females, we only used female mice at 8 weeks in subsequent experiments.

To examine if the increase of trabecular bone mass in female CD97 KO mice was due to a decreased number of osteoclasts (OCs), we performed static histomorphometric analysis. In female CD97 KO mice, there was a trend toward higher BV/TV compared to WT mice (Figure 2D), which confirmed the micro-CT analysis. This was due to significant decreases in osteoclast parameters including OC surface (Oc.S/BS, Fig. 2E), OC perimeter (N. Oc.Pm) and eroded surface (ES/BS) (data not shown) in CD97 KO compared to WT mice. We did not find a significant difference in osteoblast surface (Ob.BS) in femurs between WT and CD97 KO mice (Fig. 2F). Moreover, dynamic histomorphometric analysis revealed no significant differences in bone formation rate (Fig. 2G) and mineral apposition rate (Fig.

2H). Overall rates of bone resorption and formation in the mice were measured as levels of serum CTX and P1NP between WT and CD97 KO mice (Supplemental Figure 2.

We further employed the bone marrow stromal cell cultures to determine if CD97 was involved in osteoblast differentiation in vitro. Alkaline phosphatase activity and mineralization assays were performed in bone marrow stromal cells, which were cultured for up to 21 days in osteogenic conditions. There were no significant differences observed between cultures from WT and CD97 KO mice (data not shown), supporting our in vivo data. These data indicate that the lack of CD97 caused an increase in bone mass due to a decrease in osteoclast number without altering osteoblast number.

Osteoclastogenesis is significantly impaired in bone marrow cells of CD97-deficient mice

Our in vivo data clearly indicate that CD97 plays a positive role in osteoclast formation. To determine underlying mechanisms, we examined the effect of the CD97 null mutation on osteoclast precursor replication and number, as well as osteoclast differentiation and bone resorbing activity. We first examined the ability of bone marrow cells from WT and CD97 KO mice to form osteoclast-like cells. Bone marrow cells were cultured with M-CSF and RANKL for up to 5 days. As shown in figure 3A and B, bone marrow cells from CD97 KO mice formed significantly fewer TRAP(+) osteoclasts compared to cells from WT mice. Since bone marrow cells contain a mixed population of hematopoietic lineage and stromal cells, we also performed experiments using BMM cells. Similarly, BMM cells from CD97 KO mice showed reduced OCL formation in response to M-CSF and RANKL treatment (data not shown). Moreover, we observed that the TRAP(+) area per osteoclast, measured using the CellSens image analyzing software, was significantly reduced in the cells from CD97 KO mice compared to WT control (Fig. 3C). We investigated if CD97 modulated fusion related gene expression during osteoclast differentiation by RT-PCR. mRNA levels of DC-STAMP, Sirppr-1α (MFR, macrophage fusion receptor) and v-ATPasev0d2 were not altered in BMM cells from CD97 KO mice (data not shown). However, Sirp-1α protein expression was decreased in BMM cells from CD97 KO mice as shown in figure 3D indicating a potential mechanism that could contribute to decreased osteoclast number and size.

To determine whether defects in cell replication or migration could contribute to the reduction in OCL formation in cells from CD97 KO mice, we next examined if cells from CD97 KO mice have altered proliferation potential using a WST-1 kit and migration assay using modified Boyden chamber assay (Cell Biolabs, Inc). There was no significant difference in the number of BMM cells in the cultures from WT and CD97 KO mice (Fig. 3E). Moreover, there was no significant difference in migration between cells from WT and CD97 KO mice (data not shown). In order to measure the resorption potential of OCL formed from CD97 KO mice, we cultured bone marrow cells from WT and CD97 KO mice on collagen gels in the presence of M-CSF and RANKL. Fully differentiated multinucleated cells were collected after collagenase treatment and an equal number of cells were seeded on bone slices in the presence of M-CSF and RANKL. Cultures were maintained for 24 hrs prior to measuring the resorbed pit area per osteoclast. OCL from CD97 KO mice had smaller resorption pit area per OC than controls as shown in figure 3F. These results

indicated that the absence of CD97 led to decreased fusion as well as decreased osteoclastic resorption activity. This likely contributes to the increased trabecular bone volume observed in female CD97 KO mice.

CD97-deficient mice have a decreased number of osteoclast precursor cells

To investigate the cause of the decrease in TRAP(+) osteoclast number in cultures of bone marrow and BMM cells from CD97 KO mice in vitro and the number of osteoclasts in vivo, we examined if there is a difference in the OC precursor (OCP) population. We performed CFU-GM assays and flow cytometric analysis. Bone marrow cells from CD97 KO mice formed significantly fewer CFU-GM colonies compared to WT (Fig. 3G).

We previously reported that the majority of the early osteoclastogenic activity was found within a population of triple negative (TN) ($B220^{-}CD3^{-}CD11b^{-/lo}$) cells which were also CD115 (c-fms)^{high} and CD117 (c-kit)^{high} (population 4, P4) (39, 40). Therefore, we determined if the absence of CD97 affects this osteoclast precursor cell population in the bone marrow. As shown in figure 3H, there was a significant decrease in the P4 fraction of bone marrow from CD97 KO mice compared to WT mice. We then FACS sorted the TN c-fms^{+} osteoclast precursor population and cultured an equal number of osteoclast precursor cells for 5 days with M-CSF and RANKL. The number of TRAP(+) OCs formed in OCP from CD97 KO mice was significantly reduced when compared to WT controls (Fig. 3I) indicating a cell autonomous effect of CD97. Overall, these results indicated that CD97 KO mice contain fewer osteoclast precursor cells in bone marrow, these precursor cells have a reduced potential to differentiate into osteoclasts in vitro, and they have reduced bone resorbing activity.

CD97 up regulates osteoclastogenesis by modulating RANKL-induced NFATc1

To investigate the mechanisms by which CD97 regulates the formation of osteoclasts in response to RANKL, we first determined whether CD97 deficiency had an impact on the expression of NFATc1 and c-fos. As shown in figure 4A and B, NFATc1 and c-fos protein levels were induced by RANKL treatment in BMM cultures from WT at day 3 and peaked at day 4 of culture, while BMM cells from CD97 KO mice showed a reduction in NFATc1 and c-fos expression. These results suggest that absence of CD97 in BMM attenuates expression of transcription factors that are critical for osteoclastogenesis.

RANKL-RANK interaction initiates a variety of signaling pathways including those mediated by NF-κB, activator protein 1 (AP-1) and Ca^{2+}, and these can individually or collectively regulate NFATc1 expression. Therefore, we next investigated how CD97 modulates the NFATc1 signaling pathway in RANKL-induced BMMs. As shown in figure 4C and D, in WT BMM cells treated with RANKL, there was a progressive decrease in IκBα levels in a time-dependent manner. In contrast, IκBα levels were higher in CD97 KO cells at 3 and 7 minutes after RANKL treatment. To further confirm the effect of CD97 in the regulation of the AP-1 component, we examined the phosphorylation of c-jun in BMM cultures. As expected, phosphorylation of c-jun was induced by RANKL in BMM from WT mice but not in the cells from CD97 KO mice (Fig. 4E and F). These results suggested that

CD97 may modulate expression of NFATc1, which is a critical signal for OC differentiation, through mechanisms that involve activation of c-jun.

TNFα-induced osteoclastogenesis was significantly augmented in CD97 KO mice

Since CD97 is highly expressed in both rheumatoid arthritis and osteoarthritis synovial tissue (14), we investigated the possible role that CD97 may play during acute inflammatory stimulus, using an in vivo, localized TNFα challenge. We injected rmTNFα (0.75 μg) daily directly over the calvaria for 4 days prior to sacrifice, and TRAP(+) area per calvarial area was determined. TRAP(+) osteoclast area was significantly reduced in vehicle treated calvaria from CD97 KO mice (Fig. 5A and B), similar to our observations in femur (Fig. 2E). As expected, challenge with rmTNFα caused a significant increase in TRAP(+) osteoclast area (6 fold) in the calvaria from WT mice (Fig. 5B). Unexpectedly, in vivo TNFα treatment of CD97 KO mice greatly enhanced TRAP(+) osteoclast area (16 fold) compared to vehicle treated CD97 KO mice, indicating that the absence of CD97 accentuated the osteoclastogenic response to the inflammatory mediator, TNFα, without altering total calvarial bone volume.

To determine the cause of the increase in TRAP(+) osteoclast area, we quantified mRNA levels for various cytokines and chemokines known to enhance osteoclast differentiation, in the calvaria of TNF treated and control mice. As shown in figure 5C, the RANKL mRNA levels in calvaria from WT and CD97 KO mice were not different. TNFα treatment induced RANKL mRNA expression (1.5 fold) in calvaria from WT mice while significantly increased RANKL mRNA expression in CD97 KO mice (5 fold.) The OPG mRNA level in CD97 KO mice was elevated (2 fold) in vehicle treated calvaria when compared to WT controls (Figure 5D). Interestingly, TNFα treatment caused a significant decrease in OPG mRNA expression by 70% in calvaria from CD97 KO mice. As a result, the RANKL/OPG ratio was downregulated in CD97 KO vehicle treated calvaria compared to WT controls (Fig 5E) and TNF treatment induced RANKL/OPG ratio in calvaria from both WT (1.5 fold) and CD97 KO mice (8.8 fold). There were no differences in the TNF receptor and IL-1 receptor mRNA expression in calvaria from WT or CD97 KO mice in response to TNF treatment (Supplemental figure 3A and B). Furthermore, calvaria from WT mice treated with TNF did not display changes in the mRNA levels for any of the cytokine or chemokines assayed, with the exception of CCL3 mRNA (Fig. 5F–I). This is in marked contrast to calvaria from CD97 mutant mice, which had a robust response to TNF treatment with regard to production of cytokines and chemokines. In CD97 KO mice, mRNA levels for various cytokines and chemokines known to stimulate osteoclast differentiation, were significantly enhanced in response to TNFα treatment. These include IL-1α, CCL2, CCL3 and IL-6 (Figure 5F–I).

We subsequently measured circulating cytokine and chemokine levels in the serum from WT and CD97 KO mice using 32-multiplex kit (MILLIPLEX MAP Mouse Cytokine/Chemokine Magnetic Kit, EMD Millipore, Billerica, MA, USA). Basal cytokine and chemokine levels in serum were comparable between WT and CD97 KO mice. TNFα treatment did not cause the changes in various cytokine and chemokine levels in the serum from WT mice except for IL-6 (1.5 fold increase). TNFα treatment significantly increased the levels of IL-1β (1.6 fold) and IL-6 (19.3 fold) in the serum of CD97 KO mice (Supplemental table 1). Taken

together, bone tissue from CD97 KO mice displays an exaggerated response to acute and local inflammation. The high expression and elevated levels of soluble CD97 at sites of chronic inflammation may suggest a role for CD97 in the onset of protective immune responses.

DISCUSSION

We found a novel but contradictory role for CD97 as a positive regulator of osteoclast differentiation and function, with a protective role in response to inflammatory stimulus. In the current study we demonstrated that bone mass was significantly increased in femurs from CD97 KO female mice and that CD97 KO mice respond to inflammatory stimulus differently than WT mice. Increased trabecular bone volume was due to decreases in osteoclast parameters without altering osteoblasts and this decrease in the ability of CD97 KO cells to resorb indicates the role of CD97 is osteoclast specific in bone. Mechanistically, CD97 may modulate expression of NFATc1, which is a critical signal for osteoclast differentiation, through mechanisms that involve decreased activation of c-jun. In addition, CD97 may be involved in the fusion of osteoclasts, as Sirp-1α protein expression was downregulated in the cells from CD97 KO mice. Decreased Sirp-1α expression in CD97 KO cells may cause decreases in the size and number of osteoclasts resulting in downregulation of resorbing activity.

Though CD97 has been reported to be expressed in all types of leukocytes, epithelial, muscle, endothelial, fat and tumor cells, this study is the first to report a role for CD97 in the differentiation and the function of osteoclasts. In BMM cultures we found that CD97 mRNA expression was upregulated with RANKL treatment, while protein expression was transient. The discrepancy between mRNA and protein CD97 levels in BMM cells suggests post-transcriptional and/or post-translational regulation during osteoclast differentiation. Since multinucleated osteoclasts do not survive long on plastic once they are formed, the majority of cells left in the culture after 5 days are mainly mononuclear cells, which may express mRNA but not protein.

We also found that there was a sex specific response to the loss of CD97 in bone phenotype. This was not surprising as we and others observed several gene inactivated KO models also exhibited a sex specific bone phenotype (41–45) at the age that we examined. Females exhibited alteration in trabecular bone while males showed cortical changes. It is not clear how this sex specific response occurs at the present time. However, we attempted to explore the estrogen effect by using the ovariectomy model in CD97 KO mice. The results indicated that there was no significant difference between WT and CD97 KO female mice in bone loss after ovariectomy indicating that the disruption of estrogen was not the major factor for the sex-specific bone alteration (BV/TV-CD97 KO Sham 5.3±0.52 %; CD97 KO OVX 2.2±0.40 %). Furthermore, the alteration in the bone phenotype we observed in males and females may be stage specific since males and females develop differently in their bone growth and they differ as to when they reach their peak bone mass. It is possible that males achieve similar increased trabecular bone mass at a later time point than that shown for females at 8 weeks of age.

To examine the mechanism by which CD97 KO cells formed fewer osteoclasts in vitro and in vivo, we first measured NFATc1, a master transcription marker of osteoclast differentiation. We found that the reduction in NFATc1 expression was due to a decrease in AP-1 activation in CD97 KO cells resulting in down-regulation of osteoclast formation in CD97 KO cells. CD97 has been studied extensively in cancer cells (11, 46–48) and is known to be involved in cell invasion and proliferation and signals through Gα12/13 which increases RHO-GTP levels in prostate and thyroid cancer cells by association with lysophosphatidic acid receptor 1 (LPAR1) (46, 47). Association of CD97 and LPAR1 led to the enhanced LPA-dependent RHO and extracellular signal-regulated kinase (ERK) activation. LPA receptors are the cognate receptors for LPA and LPA modulates bone homeostasis by the activation of LPAR1 in osteoclasts (49). In this recent report, authors found that bone marrow cells from LPAR1 KO mice formed fewer osteoclasts in vitro and that this was type 1 receptor specific. Similarly, osteoclastic bone resorption was reduced in LPAR1 KO mice due to impaired podosome belts and sealing zones. Additionally, CD97 in endothelial cells interacts with Thy-1 (CD90) during inflammation to regulate the leukocyte trafficking to inflammatory sites (50). Based on these reports, it is possible that CD97 and LPAR1 may interact to modulate osteoclast formation and resorption activity.

There are two different CD97 deficient mouse models that have been generated (12, 51). In the current study we used CD97 deficient mice originating from Veninga and colleagues (12) after backcrossing with C57BL/6 mice for 7 generations. Their mouse model (12) was generated by eliminating exons 2 to 5 by recombination in 129/Ola-ES cells, while the other model replaced exons 2 to 12 with the PGKneo cassette in C57BL/6 background (51). Neither exhibited an overt phenotype, except for a mild granulocytosis. However, a granulocyte accumulation at the sites of inflammation was observed in the model used for our studies (12) while the other was significantly more resistant to listeriosis than WT mice. Moreover, CD97 deficiency in the latter model did not stimulate granulocytosis in response to peripheral inflammation (51). However, subsequent studies revealed that CD97 deficient mice, the mouse model used for our studies, had reduced arthritis activity compared to WT control mice in experimental collagen induced and K/BxN serum transfer RA models (52). In addition, a neutralizing antibody to CD97 increases the resistance to collagen induced arthritis in mice (53) and depletes granulocytes during inflammation by a Fc dependent mechanism (54).

In contrast to these previous reports, we found an acute and local inflammatory stimulus (TNFα) induced an enhanced osteoclastogenic response in CD97 KO mice. TNFα treatment augmented the expression of several cytokines and chemokines, in addition to increasing the RANKL and decreasing OPG expression in CD97 deficient mice, as summarized in figure 6. Our local TNF challenge model showed that CD97 is an essential element to suppress excessive osteoclastogenic cytokines and chemokines to stimulate osteoclastogenesis in calvaria. Since this challenge was performed over calvaria and for a short period of time, it is unlikely for other immune cells to participate in modulating osteoclastogenesis locally.

In rheumatoid arthritis and osteoarthritis, clinical signs of chronic overexpression of TNF are the swelling joints and the reduced grip strength in the diseased mice and this was due to severe synovitis with increased osteoclastic activity (55). Soluble CD97 levels in synovial

fluid are significantly enhanced in RA and OA patients, and it has been suggested that CD97 may be involved in activating proteolytic systems or in increasing synovial mass (14). However, in the current study TNF challenged mice exhibited mild enhancement of osteoclastogenesis in WT mice while CD97 KO mice showed a marked increase in osteoclastogenesis. This is possibly due to the role of CD97 in osteoclasts, since we failed to detect CD97 expression in bone marrow stromal cell cultures or in calvaria (data not shown). This supports our hypothesis that CD97 may be expressed in other cells such as macrophages or lymphocytes to respond to inflammatory signals, initially to suppress excess osteoclastogenesis. However, increased RANKL and decreased OPG expression observed in calvaria from CD97 KO mice are critical determinants for the effect on the osteoclastogenesis because CD97 may dampen the response to TNFα by other cells while enhancing RANKL response by osteoclasts. In addition cell populations involved in the rapid response to TNFα in calvaria may be different than the cells in the chronic arthritis/inflammation models. Further soluble CD97 may play different roles than the membrane-bound CD97. As previously reported, CD97 antibody, 1B2, induces neutropenia and cytokine release and depletes granulocytes only under the condition of acute inflammation rather than blocks neutrophil recruitment in mice (54). Subsequent studies revealed that the therapeutic value of CD97 antibody, 1B2, showed a similar efficacy comparable to anti-TNFα in treating arthritis and CD97 when bound to 1B2 antibody was internalized in in vitro studies (56). Altogether, these factors augmented osteoclastogenesis as an initial response to a TNF signal in CD97 KO mice.

It is possible that differences in genetic background could alter bone or inflammatory response differently. It is also possible that our TNFα treatment did not mimic long term systemic inflammation, which occurs in rheumatoid arthritis and osteoarthritis, which the majority of previous reports are based on. Additional studies are required to determine the role of CD97 in chronic inflammation as well as the mechanism of how CD97 regulates cellular responses. We demonstrated that TNFα treatment caused a significant increase in cytokine and chemokine production in the absence of CD97 and this may, in turn, enhance RANKL expression and reduce OPG expression in calvarial cells. Consequently, osteoclastogenic activity was greatly induced in the absence of CD97 as a result of enhanced cytokine and chemokine production.

Taken together, our results demonstrate that CD97 enhances osteoclast formation and thereby, lower bone mass in normal bone homeostasis. In addition, CD97 is essential to prevent over expression of osteoclasts in response to acute inflammatory stimuli, such as TNF. Unlike previous studies that examined the role of CD97 in multiple hematopoietic cells, we report the specific role that CD97 may play during osteoclastogenesis. Hence, CD97 could represent a new target to develop therapies to treat bone loss in inflammatory conditions.

Supplementary Material

Refer to Web version on PubMed Central for supplementary material.

Acknowledgments

Funding Sources: Supported by United States Public Health Service, National Institutes of Health, National Institute of Arthritis and Musculoskeletal Diseases. R01-AR055143 (SKL)

This study was supported by the U.S. Department of Health and Human Services, National Institute of Health, National Institute of Arthritis and Musculoskeletal Diseases (R01-AR055143 to SKL). We thank Drs. Joseph Lorenzo and Anne Delany (University of Connecticut Health Center) for their critical reading of the manuscript. Authors also thank Dr. Laura Haynes and Ms. Sandra Jastrzebski for their technical assistance with the multiplex assays.

References

1. Miyamoto T, Suda T. Differentiation and function of osteoclasts. Keio J Medicine. 2003; 52:1–7.
2. Miyamoto T, Ohneda O, Arai F, Iwamoto K, Okada S, Takagi K, et al. Bifurcation of osteoclasts and dendritic cells from common progenitors. Blood. 2001; 98:2544–54. [PubMed: 11588053]
3. Wong B, Rho J, Arron J, Robinson E, Orlinick J, Chao M, et al. TRANCE is a novel ligand of the tumor necrosis factor receptor family that activates c-jun N-terminal kinase in T cells. J Biological Chemistry. 1997; 272:25190–4.
4. Yasuda H, Shima N, Nakagawa N, Yamaguchi K, Kinosaki M, Mochizuki S, et al. Osteoclast differentiation factor is a ligand for osteoprotegerin/osteoclastogenesis-inhibitory factor and is identical to TRANCE/RANKL. Proceedings of National Academy of Sciences USA. 1998; 95:3597–602.
5. Dougall W, Glaccum M, Charrier K, Rohrbach K, Brasel K, Smedt TD, et al. RANK is essential for osteoclast and lymph node development. Gene Development. 1999; 13:2412–24. [PubMed: 10500098]
6. Kim Y, Sato K, Asagiri M, Morita I, Soma K, Takayanagi H. Contribution of nuclear factor of activated T cells c1 to the transcriptional control of immunoreceptor osteoclast-associated receptor but not triggering receptor expressed by myeloid cells-2 during osteoclastogenesis. J Biological Chemistry. 2005; 280:32905–13.
7. McKnight A, Gordon S. The EGF-TM7 family: unusual structures at the leukocyte surface. J Leukocyte Biology. 1998; 63:271–80.
8. Eichler W, Aust G, Hamann D. Characterization of an early activation-dependent antigen on lymphocytes defined by the monoclonal antibody BL-Ac(F2). Scand J Immunol. 1994; 39(1):111–5. [PubMed: 8290889]
9. Eichler W, Hamann J, Aust G. Expression characteristics of the human CD97 antigen. Tissue Antigens. 1997; 50(5):429–38. [PubMed: 9389316]
10. Jaspars L, Vos W, Aust G, Lier Rv, Hamann J. Tissue distribution of the human CD97 EGF-TM7 receptor. Tissue Antigens. 2001; 57:325–31. [PubMed: 11380941]
11. Steinert M, Wobus M, Boltze C, Schȍtz A, Wahlbuhl M, Hamann J, et al. Expression and regulation of CD97 in colorectal carcinoma cell lines and tumor tissues. American J Pathology. 2002; 161:1657–67.
12. Veninga H, Becker S, Hoek R, Wobus M, Wandel E, Kaa Jvd, et al. Analysis of CD97 expression and manipulation : Antibody treatment but not gene targeting curtails granulocyte migration. J Immunology. 2008; 181:6574–83. [PubMed: 18941248]
13. Van Pel M, Hagoort H, Hamann J, Fibbe W. CD97 is differentially expressed on murine hematopoietic stem- and progenitor cells. Haematologica. 2008; 93:1137–44. [PubMed: 18603564]
14. Hamann J, Wishaupt J, Lier Rv, Smeets T, Breedveld F, Tak P. Expression of the activation antigen CD97 and its ligand CD55 in rheumatoid synovial tissue. Arthritis & Rheumatism. 1999; 42:650–8. [PubMed: 10211878]
15. Kop E, Matmati M, Pouwels W, Leclercq G, Tak P, Hamann J. Differential expression of CD97 on human lymphocyte subsets and limited effect of CD97 antibodies on allogeneic T-cell stimulation. Immunology Letters. 2009; 123:160–8. [PubMed: 19428565]

16. Hamann J, Stortelers C, Kiss-Toth E, Vogel B, Eichler W, Lier Rv. Characterization of the CD55 (DAF)-binding site on the seven-span transmembrane receptor CD97. European J Immunology. 1998; 28:1701–7. [PubMed: 9603477]
17. Gray J, Haino M, Roth M, Maguire J, Jensen P, Yarme A, et al. CD97 is a processed, seven-transmembrane, heterodimeric receptor associated with inflammation. J Immunology. 1996; 157:5438–47. [PubMed: 8955192]
18. Lin H, Stacey M, Saxby C, Knott V, Chaudhry Y, Evans D, et al. Molecular analysis of the epidermal growth factor-like short consensus repeat domain-mediated protein-protein interactions. J Biological Chemistry. 2001; 276:24160–9.
19. Wang T, Ward Y, Tian L, Lake R, Guedez L, Stetler-Stevenson W, et al. CD97, an adhesion receptor on inflammatory cells, stimulates angiogenesis through binding integrin counterreceptors on endothelial cells. Blood. 2005; 105:2836–44. [PubMed: 15576472]
20. Hamann J, Vogel B, Schijndel Gv, Lier Rv. The seven-span transmembrane receptor CD97 has a cellular ligand (CD55, DAF). J Experimental Medicine. 1996; 184:1185–9.
21. Kwakkenbos M, Pouwels W, Matmati M, Stacey M, Lin H, Gordon S, et al. Expression of the largest CD97 and EMR2 isoforms on leukocytes facilitates a specific interaction with chondroitin sulfate on B cells. J Leukocyte Biology. 2005; 77:112–9.
22. Qian Y, Haino M, Kelly K, Song W. Structural characterization of mouse CD97 and study of its specific interaction with the murine decay-accelerating factor (DAF, CD55). Immunology Letters. 1999; 98:303–11.
23. Hamann J, Zeventer Cv, Biji A, Molenaar C, Tesselaar K, Lier Rv. Molecular cloning and characterization of mouse CD97. International immunology. 2000; 12:439–48. [PubMed: 10744645]
24. Lam J, Takeshita S, Barker J, Kanagawa O, Ross F, Teitelbaum S. TNF-alpha induces osteoclastogenesis by direct stimulation of macrophages exposed to permissive levels of RANK ligand. J Clin Invest. 2000; 106(12):1481–8. [PubMed: 11120755]
25. Abu-Amer Y, Ross F, Edwards J, Teitelbaum S. Lipopolysaccharide-stimulated osteoclastogenesis is mediated by tumor necrosis factor via its P55 receptor. J Clin Invest. 1997; 100(6):1557–65. [PubMed: 9294124]
26. Kobayashi K, Takahashi N, Jimi E, Udagawa N, Takami M, Kotake S, et al. Tumor necrosis factor alpha stimulates osteoclast differentiation by a mechanism independent of the ODF/RANKL-RANK interaction. J Exp Med. 2000; 191(2):275–86. [PubMed: 10637272]
27. Wei S, Kitaura H, Zhou P, Ross F, Teitelbaum S. IL-1 mediates TNF-induced osteoclastogenesis. J Clinical Investigation. 2005; 1152:282–90.
28. Zhang Y, Heulsmann A, Tondravi M, Mukherjee A, Abu-Amer Y. Tumor necrosis factor-α (TNF) stimulates RANKL-induced osteoclastogenesis via coupling of TNF type I receptor and RANK signaling pathways. J Biological Chemistry. 2001; 276:563–8.
29. Wong M, Ziring D, Korin Y, Desai S, Kim S, Lin J, et al. TNFalpha blockade in human diseases: mechanisms and future directions. Clin Immunol. 2008; 126(2):121–36. [PubMed: 17916444]
30. Kotake S, Nanke Y. Effect of TNFα on osteoblastogenesis from mesenchymal stem cells. Biochim Biophys Acta. 2014; 1840(3):1209–13. [PubMed: 24361610]
31. Clohisy D. Could apoptosis be responsible for localized imbalances in bone cell homeostasis? J Lab Clin Medicine. 1999; 134(3):190–1.
32. Lee S, Lorenzo J. Parathyroid hormone stimulates TRANCE and inhibits osteoprotegerin messenger ribonucleic acid expression in murine bone marrow cultures: correlation with osteoclast-like cell formation. Endocrinology. 1999; 140:3552–61. [PubMed: 10433211]
33. Akatsu T, Tamura T, Takahashi N, Udagawa N, Tanaka S, Sasaki T, et al. Preparation and characterization of a mouse osteoclast-like multinucleated cell population. Journal of Bone and Mineral Research. 1992; 7:1297–306. [PubMed: 1281605]
34. Shuto T, Kukita T, Hirata M, Jimi E, Koga T. Dexamethasone stimulates osteoclast-like cell formation by inhibiting granulocyte-macrophage colony-stimulating factor production in mouse bone marrow cultures. Endocrinology. 1994; 134:1121–6. [PubMed: 8119150]
35. Menaa C, Kurihara N, Roodman G. CFU-GM-derived cells form osteoclasts at a very high efficiency. Biochemical Biophysical Research Communication. 2000; 267:943–6.

36. Bouxsein M, Boyd S, Christiansen B, Guldberg R, Jepsen K, Müller R. Guidelines for assessment of bone microstructure in rodents using micro–computed tomography. Journal of Bone and Mineral Research. 2010; 25:1468–86. [PubMed: 20533309]
37. Parfitt A, Drezner M, Vlorieux F, Kanis J, Malluche H, Meunier P, et al. Bone histomorphometry:stardization of nomenclature, symbols, and units. Report of the ASBMR Histomorphometry Nomenclature Committee. J Bone Mineral Research. 1987; 2:595–610.
38. Roguljic H, Matthews B, Yang W, Cvija H, Mina M, Kalajzic I. In vivo identification of periodontal progenitor cells. J Dent Res. 2013; 92:709–15. [PubMed: 23735585]
39. Jacquin C, Gran D, Lee S, Lorenzo J, Aguila H. Identification of multiple osteoclast precursor populations in murine bone marrow. J Bone and Mineral Research. 2006; 21:67–77.
40. Jacome-Galarza C, Lee S, Lorenzo J, Aguila H. Identification, characterization and isolation of a common progenitor for osteoclasts, macrophages and dendritic cells from murine bone marrow and periphery. J Bone and Mineral Research. 2013; 28:1203–13.
41. Lee S, Kalinowski J, Jacquin C, Adams D, Gronowicz G, Lorenzo J. Interleukin-7 influences osteoclast function *in vivo* but is not a critical factor in ovariectomy-induced bone loss. J Bone Mineral Research. 2006; 21:695–702.
42. Aguila H, Mun S, Kalinowski J, Adams D, Lorenzo J, Lee S. Osteoblast-specific overexpression of human interleukin-7 rescues the bone mass phenotype of interleukin-7 deficient female mice. J Bone and Mineral Research. 2012; 27:1030–42.
43. Mun S, Won H, Hernandez P, Aguila H, Lee S. Deletion of CD74, a putative MIF receptor, in mice enhance osteoclastogenesis and decreases bone mass. J Bone and Mineral Research. 2013; 28:948–59.
44. Martineau C, Martin-Falstrault L, Brissette L, Moreau R. Gender- and region-specific alterations in bone metabolism in Scarb1-null female mice. J Endocrinology. 2014; 222(2):277–88. [PubMed: 24928939]
45. Martineau C, Martin-Falstrault L, Brissette L, Moreau R. The atherogenic Scarb1 null mouse model shows a high bone mass phenotype. American J Physiol Endocrinol Metab. 2014; 306:E48–E57.
46. Ward Y, Lake R, Yin J, Heger C, Raffeld M, Goldsmith P, et al. LPA receptor heterodimerizes with CD97 to amplify LPA-initiated Rho-dependent signaling and invasion in prostate cancer cells. Cancer Research. 2011; 71:7301–11. [PubMed: 21978933]
47. Ward Y, Lake R, Martin P, Killian K, Salerno P, Wang T, et al. CD97 amplifies LPA receptor signaling and promotes thyroid cancer progression in a mouse model. Oncogene. 2013; 32:2726–38. [PubMed: 22797060]
48. Davies J, Lin H, Stacey M, Yona S, Chang G, Gordon S, et al. Leukocyte adhesion-GPCR EMR2 is aberrantly expressed in humanh breast carcinomas and is associated with patient survival. Oncology Reports. 2011; 25:619–27. [PubMed: 21174063]
49. David M, Machuca-Gayet I, Kikuta J, Ottewell P, Mima F, Leblanc R, et al. Lysophosphatidic acid receptor type 1 (LPA1) plays a functional role in osteoclast differentiation and bone resorption activity. J Biol Chem. 2014; 289(10):6551–64. [PubMed: 24429286]
50. Wandel E, Saalbach A, Sittig D, Gebhardt C, Aust G. Thy-1 (CD90) is an interacting partner for CD97 on activated endothelial cells. J Immunol. 2012; 188(3):1442–50. [PubMed: 22210915]
51. Wang T, Tian L, Haino M, Gao J-L, Laki R, Ward Y, et al. Improved antibacterial host defense and altered peripheral granulocyte homeostasis in mice lacking the adhesion class G protein receptor CD97. Infection and Immunity. 2007; 75:1144–53. [PubMed: 17158902]
52. Hoek R, Launay Dd, Kop E, Yilmaz-Elis A, Lin F, Reedquist K, et al. Deletion of either CD55 or CD97 ameliorates arthritis in mouse models. Arthritis & Rheumatism. 2010; 62:1036–42. [PubMed: 20131275]
53. Kop E, Adriaansen J, Smeets T, Vervoordeldonk M, Lier Rv, Hamann J, et al. CD97 neutralisation increases resistance to collagen-induced arthritis in mice. Arthritis Research & Therapy. 2006; 8:R155. [PubMed: 17007638]
54. Veninga H, Groot Dd, McCloskey N, Owens B, Dessing M, Verbeek J, et al. CD97 antibody depletes granulocytes in mice under conditions of acute inflammation via a Fc receptor-dependent mechanism. J Leukocyte Biology. 2011; 89:413–21.

55. Hayer S, Steiner G, Görtz B, Reiter E, Tohidast-Akrad M, Amling M, et al. CD44 is a determinant of inflammatory bone loss. J Experimental Medicine. 2005; 201:903–14.

56. de Groot D, Vogel G, Dulos J, Teeuwen L, Stebbins K, Hamann J, et al. Therapeutic antibody targeting of CD97 in experimental arthritis: the role of antigen expression, shedding, and internalization on the pharmacokinetics of anti-CD97 monoclonal antibody 1B2. J Immunol. 2009; 183(6):4127–34. [PubMed: 19717518]

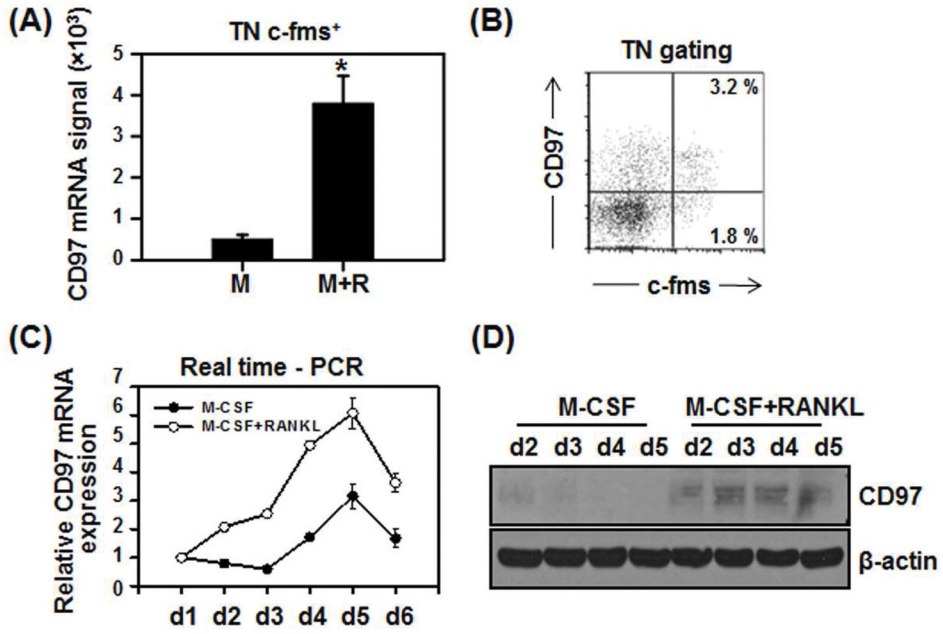

Figure 1.

RANKL induced CD97 expression during osteoclastogenesis. A) TN c-fms+ cells from WT mice were cultured for 4 days with M-CSF in the absence or presence of RANKL before RT-PCR was performed. B) Flow cytometric analysis of bone marrow cells indicates the expression of CD97 in osteoclast precursor cells (~3.2 %). C) BMM cells were cultured for up to 6 days either with M-CSF or M-CSF and RANKL. RNA was converted to cDNA and real-time PCR was performed D) CD97 protein expression was transiently detected in RANKL treated BMM cultures at day 2 and peaked at day 3. Values represent mean±SEM. *, Significant effect of RANKL treatment, $p<0.05$. TN: triple negative, $B220^{-}CD3^{-}CD11b^{-/lo}$.

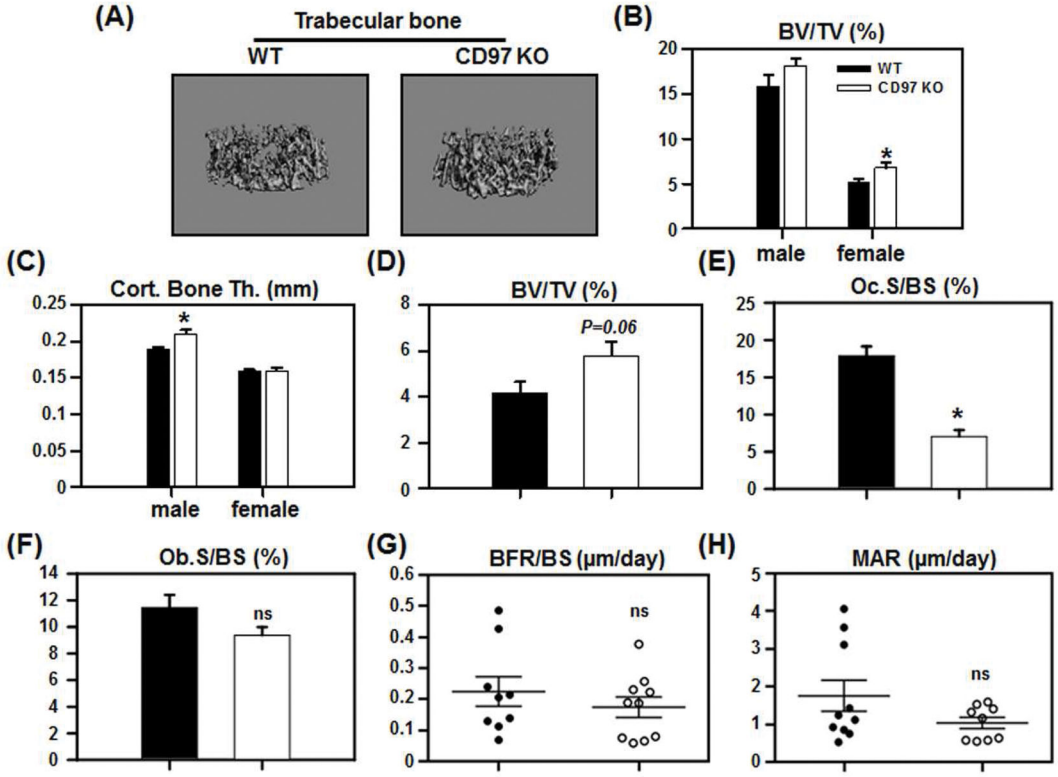

Figure 2.

CD97 KO mice had increased bone mass with decreased osteoclast number. (A–C) The femurs from WT and CD97 KO mice were analyzed by micro-CT. A) Representative images of trabecular bone from WT and CD97 KO female mice. B) Trabecular bone volume (BV/TV); C) Cortical bone thickness. (D–F) Static histomorphometric analysis. The femurs from WT and CD97 KO female mice were sectioned, stained for H&E and TRAP and were analyzed by Osteomeasure. D) Trabecular bone volume (BV/TV); E) osteoclast surface (Oc.S.BS); F) osteoblast surface (Ob.S/BS). (G–H) Dynamic histomorphometric analysis. Mice were injected with calcein 9 and 2 days prior to sacrifice. Frozen sections from the femurs of WT and CD97KO mice were evaluated. (G) Bone formation rate per bone surface; (H) Mineral apposition rate. Values represent mean SEM. N=6–11. *, Significant effect of CD97 KO mice, $p<0.05$. ns: not significant.

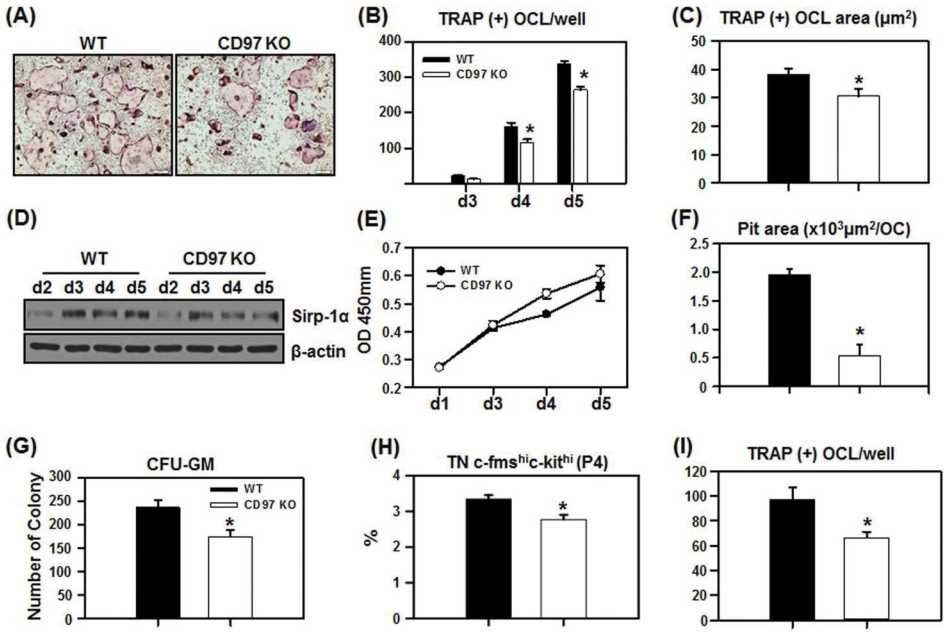

Figure 3.

Bone marrow cells from CD97 KO mice have reduced ability to form osteoclasts and reduced resorption activity. Bone marrow cells from WT and CD97 KO mice were cultured with M-CSF and RANKL (30 ng/ml) for duration as indicated. A) Representative micrographs of cultures for 4 days. B) Bone marrow cells from WT and CD97 KO mice were cultured for up to 5 days in the presence of M-CSF and RANKL. TRAP(+) OCL per well was scored. C) BMM cells from WT or CD97 KO mice were cultured for 5 days and the size of the osteoclasts were measured using the CellSens image analyzing software. D) Attenuation of Sirp-1α protein expression in BMM cultures from CD97-deficient mice. E) Cell proliferation assay was performed using WST-1 reagent. BMM cells were plated in a 96 well plate and treated with M-CSF and RANKL for up to 5 days prior to the assay. F) Bone marrow cells from WT and CD97 KO mice were cultured with M-CSF and RANKL on collagen gels and an equal number of fully differentiated multinucleated cells were seeded on bone slices for 24 hrs and the area of resorbed pit per osteoclast was measured. CD97 KO mice have decreased osteoclast precursors. G) CFU-GM assay. Bone marrow cells from WT and CD97 KO mice were cultured in semisolid methylcellulose to examine the number of osteoclast precursor cells in the presence GM-CSF for 7 days and the number of colonies containing more than 40 cells were counted. H) P4 (TN c-fms[CD115]^{hi}c-kit[CD117]^{hi}) population in total bone marrow cells of WT and CD97 KO mice were measured by flow cytometry. I) FACS sorted cell (TN c-fms^{+}) from long bones (femurs and tibia) were cultured with M-CSF and RANKL (30 ng/ml) for 5 days prior to TRAP(+) staining. Experiments were performed at least three times and the representative experiment is shown. TN: B220^{-}CD3^{-}CD11b$^{-/lo}$. Values represent mean±SEM. *, Significant effect of CD97 KO mice, $p<0.05$.

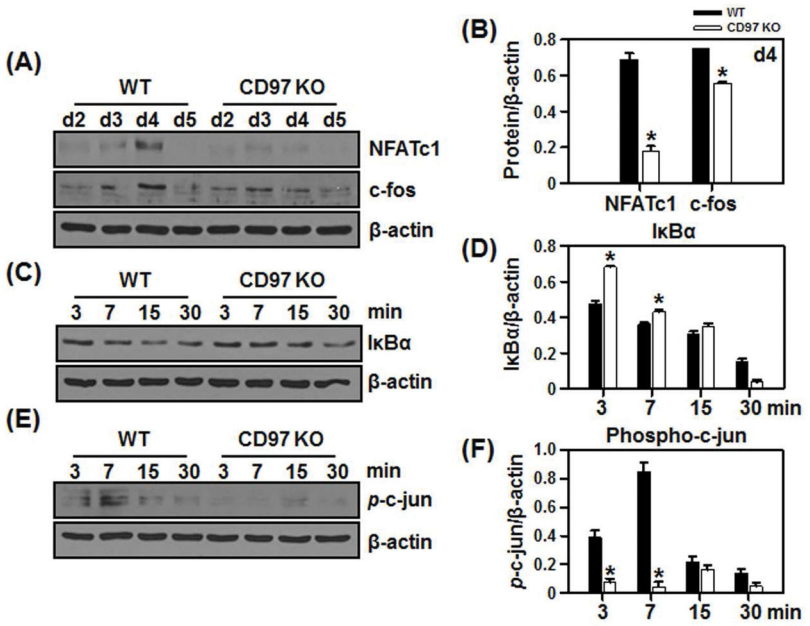

Figure 4.

Attenuation of NFATc1 and AP-1 expression in BMM cultures from CD97-deficient mice. BMM cells from WT and CD97KO mice were cultured with M-CSF and RANKL for the period indicated. Total proteins were isolated, equal amount of whole cell lysates were loaded and analyzed for NFATc1, c-fos (A) protein expression in the presence MCSF and RANKL. B) Bar graphs indicated the densitometric analysis of multiple experiments measuring NFATc1 and c-fos protein levels at day 4. C–F) BMM cells from WT and CD97 KO mice were cultured with M-CSF alone for 3 days before RANKL was added as indicated. C–F) Western blot was performed to detect the C) IκBα and E) phospho-c-jun. Bar graphs indicate the densitometric analysis of multiple experiment measuring D) IκBα and F) p-c-jun protein levels normalized to β-actin. Values represent mean±SEM. *, Significant effect of CD97 KO mice, $p<0.05$.

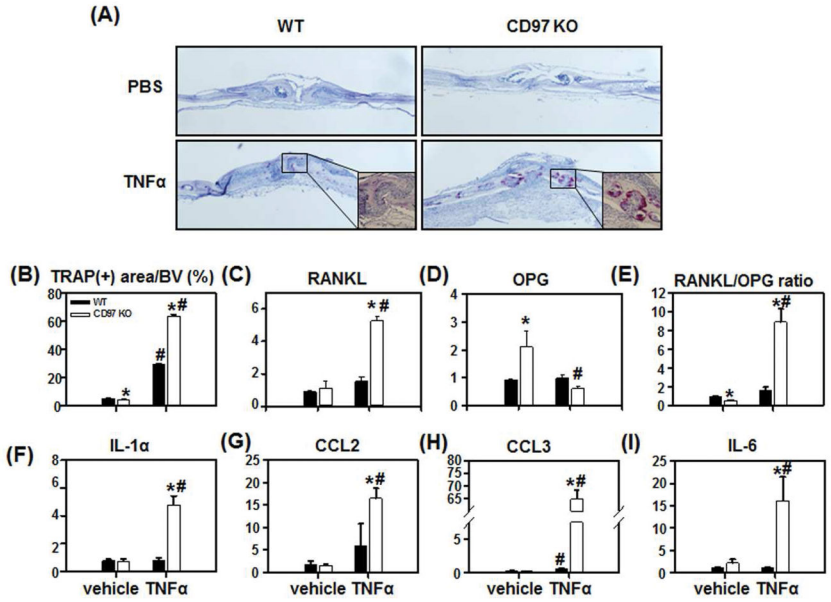

Figure 5.

CD97 deficiency enhanced TNFα induced osteoclastogenesis in vivo. WT and CD97 KO female mice were injected over calvaria with PBS or TNF (0.75 μg) daily for 4 days. A) Representative micrographs of TRAP-stained histological sections of calvaria. B) Percentage of TRAP(+) osteoclast surface per bone volume. C-I Total RNA from calvaria of WT and CD97 KO mice was extracted. mRNA expression was expressed as fold change compared to control group. C) RANKL, D) OPG, E) RANKL/OPG mRNA ratio, F) IL-1α, G) CCL2, H) CCL3, and I) IL-6 mRNA expression in calvaria by real-time PCR. Experiments were performed at least three times and the pooled data are shown. Values represent mean±SEM. *, Significant effect of CD97 KO mice; #, Significant effect of rmTNFα treatment, $p<0.05$.

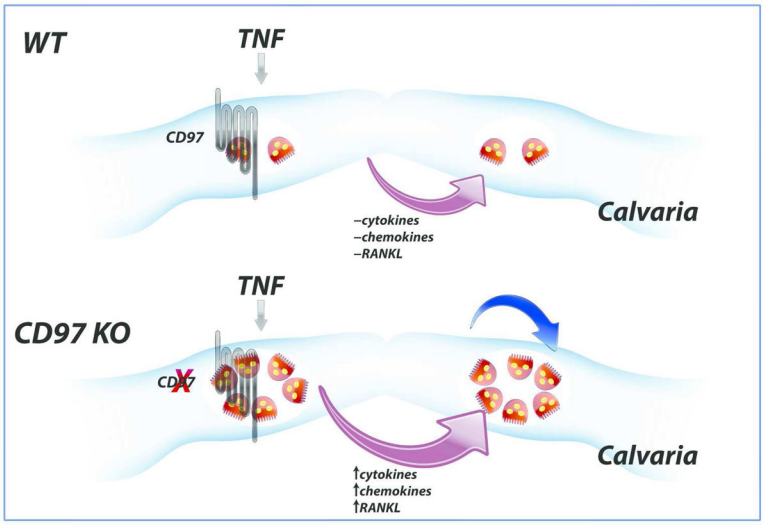

Figure 6.

Model of short term acute and local inflammatory stimulus (TNFα)-induced osteoclastogenesis in CD97 KO mice. TNFα treatment augmented the expression of CD97 to suppress excess osteoclastogenesis in WT mice while TNF treatment markedly enhanced various cytokines and chemokine in addition to increasing the RANKL and reducing OPG expression in the absence of CD97 to increase in osteoclast formation in bone marrow cavity of calvaria. Blue arrow indicates the possible cell autonomous effect of osteoclasts in response to TNFα.